OPEN ACCESS

Precision Medicine Communications
DOI: 10.55627/pmc.003.001.0300

Research Article

Exploring the Potential of Drug Repurposing: Detection of Cystic Fibrosis Transmembrane Conductance Regulator as a Biomarker in Breast Cancer Patients

Sobia Rafiq[1], Sana Khan[1], Shumaila Wazir[1], Haseena Nawaz[1], Mah Muneer Khan[2], Sadia Fatima[1], Babar Jamal[3], Asif Ali[4,5*], Ishaq N. Khan[1,6*]

[1]Institute of Basic Medical Sciences, Khyber Medical University, Peshawar 25120, Pakistan
[2]Department of Surgery, Khyber Teaching Hospital, Peshawar 25120, Pakistan
[3]Department of Biological Sciences, National University of Medical Sciences, Rawalpindi, Pakistan
[4]Institute of Pathology and Diagnostic Medicine, Khyber Medical University, Peshawar 25120, Pakistan
[5]College of Medicine, Gulf Medical Univesity, Ajman, United Arab Emirates
[6]Texas A&M Health Science Center, Joe H. Reynolds Medical Build, College Station, TX 77843, United States
***Correspondence**: isaackhan1@tamu.edu (INK), draliasif7@gmail.com (AA)

Abstract

Despite the advancements in cancer treatment and the benefits of personalized medicine, breast cancer (BC) remains a significant health concern. Also, conventional treatment options are costly and often associated with severe side effects, highlighting the need to identify new biomarkers and innovative treatment strategies for BC. Drug repurposing presents an approach that expands the therapeutic window further to mitigate the financial burden and minimize the potential harm caused by existing anticancer drugs. In the present study, we aim to suggest noncancerous FDA-approved drugs for repurposing, through molecular docking studies in BC, after their target cystic fibrosis transmembrane conductance regulator protein (CFTR) detection in BC. We used a drug repurposing approach to identify the target protein CFTR and drugs that target CFTR. MOE (molecular operating environment) was used to analyze the interaction between CFTR and its targeting drugs. For experimental work, we did Immunofluorescence staining on BC tissue. We found that glyburide and tezacaftor were the top antagonist and agonists, respectively. We detected CFTR expression in all ten samples except Triple-Negative Breast Cancer (TNBC). CFTR and estrogen receptor alpha co-expressed at 6.78%, suggesting a potential relationship. High-grade tumors showed CFTR low expression, hinting at CFTR down-regulation and its role in tumor aggressiveness. Our study is a preliminary step towards in-vitro and in-vivo experiments on repurposing CFTR-targeting drugs in BC. Glyburide may inhibit CFTR's role in estrogen production, while tezacaftor can enhance CFTR action to overcome tumor aggressiveness.

Keywords: Breast cancer, drug repurposing, CFTR, glyburide, tezacaftor

1. Introduction

The persistent toxicity issues associated with market-available cancer drugs have necessitated the development of an alternative strategy for therapeutic purposes of breast cancer (BC). Despite landmark discoveries and progress in oncological medicines, BC is still the leading cause of death worldwide (Antoszczak et al. 2020; You et al. 2019). While standard treatment options have improved patients' lifetimes and made breakthroughs in radiotherapy and chemotherapeutic treatments, they often prove ineffective for advanced-stage cancer patients(Cao et al. 2021). The traditional drug discovery process is always time-consuming and expensive. It usually takes 10–15 years and 0.8–1.5 billion dollars,

along with a high loss rate. In contrast, drug repurposing is a more pragmatic approach that may reduce the drug development period to 6.5 years and research costs to $300 million. Earlier, the repurposing was serendipitous. However, serendipity cannot be used as a routine method. The rapid growth of computing power is essential in drug repurposing studies by utilizing cheminformatics, bioinformatics, systems biology, and computational methods. As a computational approach, molecular docking is vital in identifying hits, their optimization, drug repositioning, and checking their interactions. Molecular docking significantly reduces cost and time by selecting only the promising molecules and leading them to the in-vitro phase. (Rangel-Vega et al. 2015). Docking also gives information about the activity and interaction of drugs with proteins by predicting binding energy values of different binding poses. Among many different poses, a pose with low binding energy is selected to obtain the optimized orientation of the ligand and target complex (Ahmed and Alkali 2019).

Recent research has recognized the critical role of ion channels in tumors, making them attractive molecular targets for drug action. Various ion channels of cell membranes and organelles regulate tumor cell proliferation, apoptosis, invasion, and migration; some ion channels, such as chloride, are called oncogenic channels. Glycoprotein cystic fibrosis transmembrane conductance regulator protein, shortly known as CFTR, is one such protein. CFTR belongs to the ABCC family, specifically ABCC7, within the larger group of forty-eight ABC proteins categorized into seven. It expresses on the epithelial surface of the stomach, nasal cavity, and lungs, which are involved in fluid secretion, i.e., tears, sweat, and mucus (Locher 2016; Meng et al. 2019). It allows chloride ions to pass passively. Having an essential role in ion conduction, CFTR regulates the viscosity of liquid secretion and pH regulation and maintains secretory volume (Toprak, Davis, and Rosenfeld 2019). Dysfunction of CFTR results in the inability to export chloride ions, leading to the retention of water within cells, causing the production of abnormally thick fluids. CFTR imbalances can lead to conditions such as diarrhea, constipation, and lung abnormalities (Quintana-Gallego, Delgado-Pecellín, and Acuña 2014).

CFTR expresses on the epithelial cell surface from where most cancers originate (Zhu et al. 2017). Accumulating evidence has indicated the association of inflammatory pathways and inflammation-related cancers with genetic variations in the CFTR gene (Cohen and Prince 2012). Also, there is a suggestion that CFTR interacts with a protein class (kinases) related to cancer (Muriithi et al. 2020). Ting Zhang and his colleagues recently reported CFTR involvement in regulating a transcriptional factor called NF-κB. Overexpression of this protein will lead to aberrant activation of a complex called the *uPA*/*uPAR* axis, which is critical in epithelial-mesenchymal transition (EMT). As a result, cancer cells become motile through loss of integrity and tight junction. (Zhang et al. 2013), while normalizing CFTR levels reversed these activities (Liu et al. 2020). CFTR is also involved in estrogen production in ovaries through the FSH-stimulated signaling pathway. This finding of CFTR-based amplification of hormonal response may extend to other organs (Chen et al. 2012). Another study reported CFTR over-expression to be involved in the development and progression of ovarian cancer. Furthermore, the down-regulation of CFTR suppressed ovarian cancer cells' aggressively malignant behaviors in-vitro and in-vivo. Additionally, genetic mutations in CFTR have also been found to be associated with a lower risk of several other carcinomas, i.e., lung cancer (Li et al. 2010), prostate cancer (Qiao et al. 2008), and melanoma (Warren et al. 1991).

Despite all these observations, CFTR expression in different BC types remains inconclusive. Given CFTR's involvement in estrogen production, its role in ovarian cancer, and its association with EMT, it is reasonable to investigate CFTR expression in different BC types and high-grade tumors. As mentioned, normalizing CFTR expression suppresses aggressive tumors; therefore, we aim to suggest FDA-approved noncancerous antagonists and agonists, respectively, for target CFTR through docking studies to combat aggressive tumors. Our results demonstrate varied CFTR expression in different BC subtypes and suggest promising repurposing candidates for BC treatment.

2. Methodology

2.1. Data collection

The study design involved both computational and experimental approaches. For experimental work, the data was collected from BC patients of Khyber Teaching Hospital, surgical ward B, after their informed consent. Ten high-grade breast tumor tissues (formalin/dry), after Modified Radical Mastectomy (MRM), were taken to detect biomarker protein CFTR. In the computational aspect of the study, a database called repurposing hub (Bairoch et al. 2005) which provides information on drugs that can be repurposed for cancer, was searched. Drug targets were identified from the drug bank (Thul and Lindskog 2018), while protein localizations were found through online databases called Gene card, and Uniport (Krisnamurti and Fatchiyah 2019). Protein expression in BC was searched using the human protein atlas (Thul and Lindskog 2018). A total of one hundred drugs were searched, and their respective targets were obtained.

2.2. Computational Work

A comprehensive screening process of 100 drugs was conducted to obtain a single drug of interest: tezacaftor. The results are documented in supplementary tables 1, 2, and 3. The same hub was used to obtain a list of 23 drugs targeting CFTR. However, only the 11 drugs that had received FDA approval were considered for further analysis. The structural information of tezacaftor was obtained from the ZINC15 database, while the structural data of CFTR was retrieved from the Protein Data Bank. Out of the 11 relevant CFTR protein structures, the most suitable one was selected using an inclusion-exclusion criterion. The selection was based on criteria such as the presence of suitable binding sites, a specific mutant type, a lower resolution number (e.g., 1Å), and a low count of missing residues.

2.2.1. Drug and Protein Structures Preparation in MOE

The protein structure was refined by removing solvents and extraneous ligands, except for Ivacaftor, and hydrogen atoms were added through the protonation of the 3D structure. The drugs were prepared in a molecular operating environment (MOE) by minimizing their energy and applying 3D protonation. The prepared protein structure, as well as the active sites of the protein, were validated and identified using various methods such as PDB, Discovery Studio, and literature search. The results, including the prepared protein structure and the isolated binding pocket, can be seen in Figure 1.

In the docking process, all the drugs were repositioned to the active site, which required determining the orientation of the active site by isolating it from the protein structure. This isolated binding pocket, shown in Figure 1, was obtained by removing the protein backbone and retaining only the pocket region. A self-docking step was performed using RMSD (root

mean square deviation) to validate the docking protocol. RMSD measures the average distance between the atoms of two superimposed structures. In this case, an experimental structure of a protein-ligand complex (602P) obtained from the PDB with a 3D structure was obtained. Self-docking of the complex was performed with the same drug to compare the docking pose and active residues with the experimental structure. A low RMSD value indicates higher accuracy, and 2Å or less is generally preferred. To select the most suitable drug(s) from the pool of 11 options, molecular docking was performed using the MOE, ChemCompd 2009.10 software.

2.2.2. Molecular Docking

All the prepared drugs were docked against prepared protein, and the results were saved as 'result dock.mdb'. The obtained file was sorted, based on s-scores or binding scores, to obtain both agonist and antagonist for further analysis. The graph is shown in Figure 1 of the results. Each drug was individually analyzed against the active sites, and their 3D images were saved in JPEG format. MOE and Discovery Studio Visualizer 19 were used to analyze these images, allowing for the observation of the type of bonding between drug and protein. 3D images are presented in Figure 2.

2.3. Experimental Work

2.3.1. Immunofluorescence Staining

Microtome and cryotome cutting of 4-5 µm was done to prepare FFPE blocks and Cryomolds. Antigen retrieval was performed on the FFPE samples using citrate buffer at pH 6.0 and a temperature of 95 °C for 15 minutes. For CFTR expression analysis, mouse monoclonal anti-CFTR (Abcam) primary antibody (100ul), with red-colored goat anti-mouse IgG secondary antibody (500ul), was used. Anti-estrogen receptor alpha and oct3/4 (Abcam) were used as transcriptional factors (TFs) and were visualized using green color.

After washing the slides with PBS, Permeabilization was done with PBSt using 0.1% Tr-X in the desired amount of PBS. This step was followed by the blocking step using a blocking buffer (5% of FBS, 0.1 % of tween-20/triton –X). Primary antibodies were used at concentration 1:200. Slides were incubated overnight with the primary antibody in a humidified chamber at 4°C. Subsequently, secondary antibody application was done at 1:500 for 1 hour in the darkroom.

For nuclei visualization, slides were stained with DAPI. A few drops of mounting medium were added to the slides. A cover slip was placed on stained tissue, sealed with varnish, and allowed to dry.

The slides were examined under a fluorescent microscope. The images obtained from all three channels (CFTR, TFs, and DAPI) were merged using Adobe Photoshop to obtain RGB images. Nuclei were counted manually as well as using image analysis software like Image J.

2.4. Statistical Analysis

Nuclei counting and expression quantification were performed using both manual and automatic methods. The manual count is considered the gold standard, but since the process is laborious and error-prone, an additional count is conducted through software called Image J. This automated counting method provides precise results if the smallest nuclei are accurately identified. Based on these counts, the percentages of expressed biomarkers were calculated. The mean value was obtained by averaging the manual and automated counts results. Standard deviation and standard error mean were also calculated to assess the variability and precision of the data.

a. Protein structure obtained from PDB

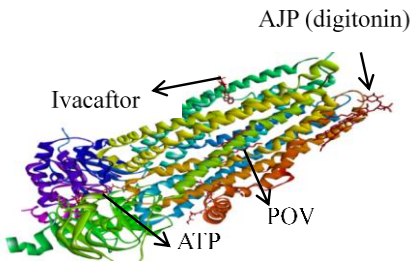

b. Prepared protein structure

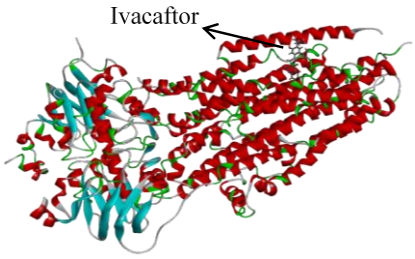

c. Isolated binding site

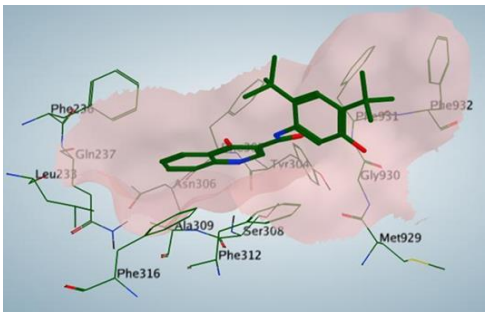

d. Self-docking

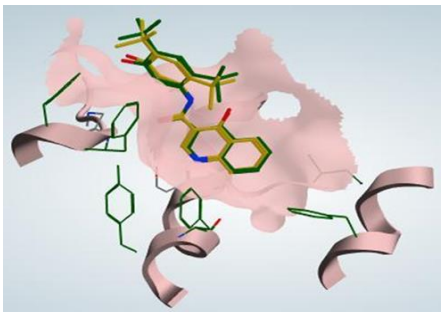

Complex	Mseq	S	rmsd_refine	E_conf	E_place	E_score1	E_refine
Nimotop- 6O2P	1	-17.8915	2.2874563	62.09301	-65.249161	-9.6207924	-17.89159
Ibuprofen-6O2P	2	-12.9460	1.891748	13.302761	-72.37516	-9.5935183	-12.94600
Bumetanide- 6O2P	3	-18.2072	1.6977828	-66.70537	-82.319565	-10.591283	-18.20720
Ivacaftor- 6O2P	4	-17.4435	2.7376935	71.201447	-67.797844	-9.6485081	-17.44355
Glyburide-6O2P	5	-20.6541	2.0784447	-71.35972	-75.304138	-10.287892	-20.65414
Lumacaftor-6O2P	6	-19.1977	2.6240692	7.7875304	-70.915466	-11.809959	-19.19770
Tezacaftor- 6O2P	7	-20.0947	1.4637171	94.547791	-89.823029	-9.3920517	-20.09473
Ataluren- 6O2P	8	-17.3511	1.5716966	39.180981	-62.835728	-10.74618	-17.35110
Capsaicin-6O2P	9	-18.7858	2.2126155	-5.182867	-49.827286	-10.649638	-18.78587
Felodipine-6O2P	10	-17.2238	1.5565728	28.580969	-47.679295	-8.4980345	-17.22384
Glafenin-6O2P	11	-16.9992	2.8628409	82.911263	-66.059402	-9.5810204	-16.99929

e. Docking results

f. Docking results arrangement on the basis of binding score

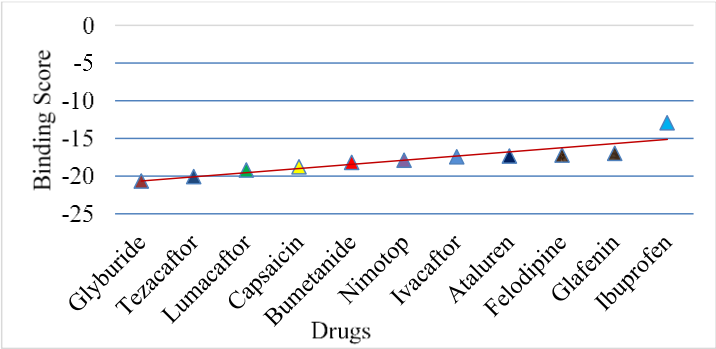

Figure 1 Molecular docking. The protein obtained from PDB was a single chain with an unknown peptide entity (UNK) and conjugated with five unique ligands, shown in red, like adenosine triphosphate and AJP (digitonin). VX7 (Ivacaftor) and Mg (magnesium). b: All the ligands except Ivacaftor (FDA-approved drug for CFTR) were removed through MOE to obtain the protein required for docking. c shows an active site first isolated, and the protein backbone was removed from the structure. Identification and isolation of active sites are vital because, behind standard ligands, many other ligands are attached, specifying many binding sites other than the standard one*(El-Hamamsy 2017)*. The following active sites remained conserved in all three methods. F932, S308, Y304, F305, F236, L233, A309, F931, G930, F312, VX71512. d. The docking protocol was validated by using RMSD. Our redocked drug was found to be almost precisely superimposed on an experimental structure with an RMSD value of 0.4531 Å. The drug in green is the experimental drug, while yellow is the same redocked drug. e. After building the ligand library and validating the protocol, the mdb file of drugs was repositioned into the isolated active site of protein through MOE software. The table mentioned above shows the results obtained from docking. f. Docking results were then arranged based on binding score/binding energy. Whenever ligands and proteins interact to form a bond, the release of energy is termed binding energy. A negative and low binding energy value shows that the complex is stable. The red line shows the trend of binding score that increases as we move from left to right.

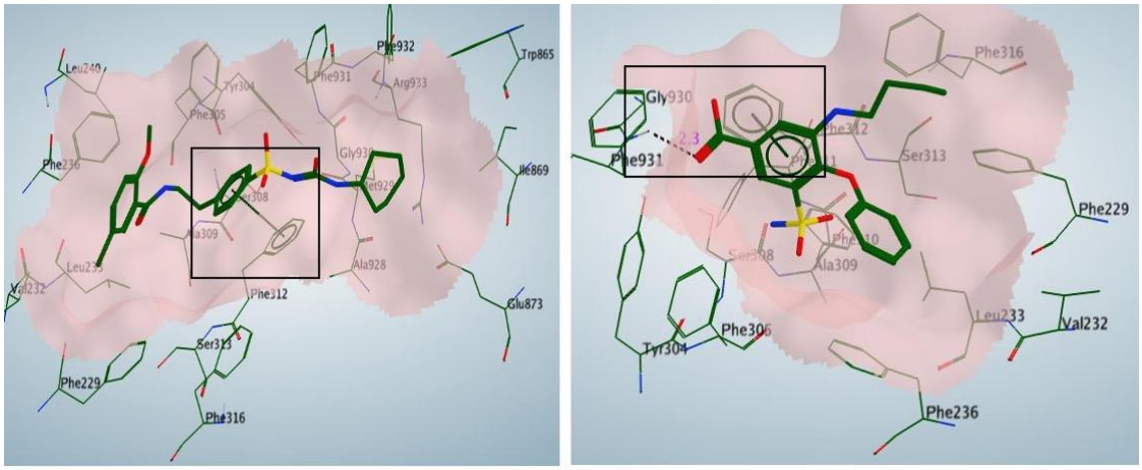

Docking antagonist results interpretation; a: glyburide-CFTR complex, b: bumetanide-CFTR complex

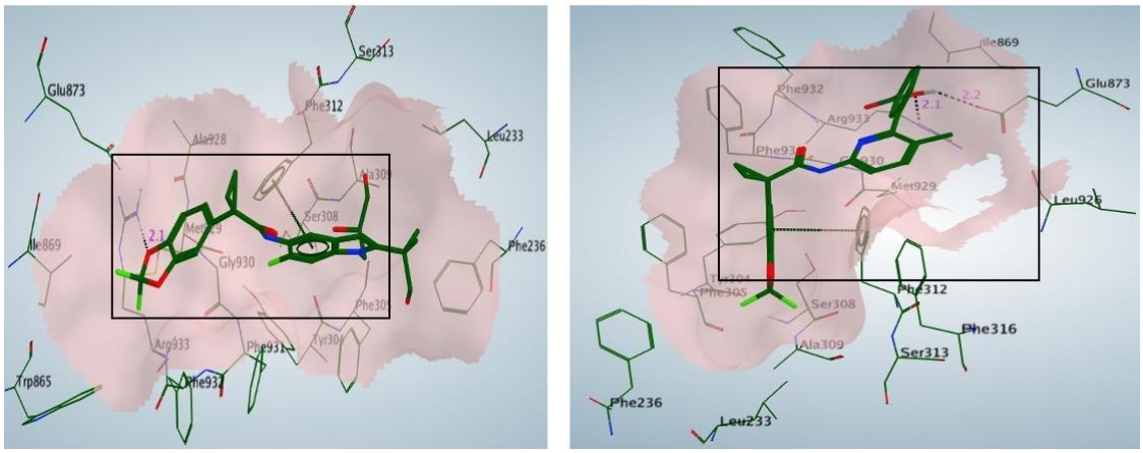

Figure 2 Docking antagonist/agonist results interpretation: a: Glyburide shows arene-arene or (pi-pi) interaction with Phe312 of CFTR, having a bond length of 4.13 Angstrom. In pi-pi interaction, one ring is electron deficient, and the other is electron rich. Both interact to form a bond by sharing their electrons, forming a stable complex. b: bumetanide shows bonding with CFTR at two points, i.e., arene-arene at Phe312, while hydrogen bond at Phe931, with bond lengths 4.13 and 2.3 angstroms, respectively. Pi-pi interaction is between two aromatic rings, one is electron deficient, and the other is electron rich. The same aromatic ring branch bearing electronegative oxygen end forms a hydrogen bond with Phe931 of CFTR. c: 3D interaction of the tezacaftor-CFTR complex showed bonding at two points, i.e., Phe312 and Arg 933. One interaction is the arene-arene or (pi-pi) interaction between Phe312 of CFTR and drugs benzene ring, with a bond length of 5.70 Angstrom. Arg933, through its NH2 forms a conventional hydrogen bond with an oxygen-bearing five-membered ring of tezacaftor having bond length 2.1Angstrom. d: CFTR binds to the lumacaftor benzene ring through its Phe312 residue having a bond length of 5.70 Angstrom. Arg933, through its NH2 forms a conventional hydrogen bond with an oxygen-bearing five-membered ring of lumacaftor, the bond length being 2.1Angstrom. Glu873, through its oxygen-bearing end, interacts with the hydrogen of CH2. Interaction is polar, and the bond length is 2.2 Angstrom.

3. Results

3.1. Computational Part

After drug-based protein identification and obtaining all the drugs that target CFTR, we prepared the protein for further analysis. The raw protein structure obtained from the Protein Data Bank (PDB) is depicted in Figure 1a. However, this structure contained several unnecessary ligands that were removed, resulting in the prepared protein structure shown in Figure 1b. To isolate the binding pocket of interest, Figure 1c illustrates the isolated binding pocket obtained by removing the protein backbone, leaving only the pocket region. The self-docked pose of the protein with the drug is shown in Figure 1d, which was used to validate the docking protocol. Figures 1e and 1f present the molecular docking results,

providing insights into the binding interactions between the drugs and the CFTR protein.

3.1.1. Docking Results

Among antagonists, glyburide-6O2p complex showed the lowest binding energy, i.e., -20.6541, followed by bumetanide, with a binding energy of -18.2072. On the other hand, among agonists, tezacaftor and lumacaftor were the top two drugs with binding energies of -20.09473 and -19.19770, respectively. The low binding free energy data also showed that these drugs form promising docked complexes with the target.

3.2. Experimental Part

3.2.1. Tumor Characteristics

As per the inclusion and exclusion criteria, ten codes were selected and processed, including both FFPE and frozen. The codes BC1, BC2, BC3, and the rest denote BC samples numbered 1, 2, 3, and so on. A table in the appendix presents all the clinical data and data generated by the Khyber Medical University (KMU) for these codes. IF staining was done on both FFPE and frozen samples. We divided the tumors into three categories, i.e., high-grade tumors (grade III), ER+ tumors, and TNBC tumors.

3.2.2. CFTR Expression in High-Grade Tumors

Five of the ten analyzed samples were identified as high-grade aggressive tumors. Histopathology reports generated by KMU confirmed this classification. The samples BC1, BC4, BC5, BC6, and BC8 corresponded to high-grade tumors. The expression of CFTR in these high-grade tumors is summarized in Figure 3.

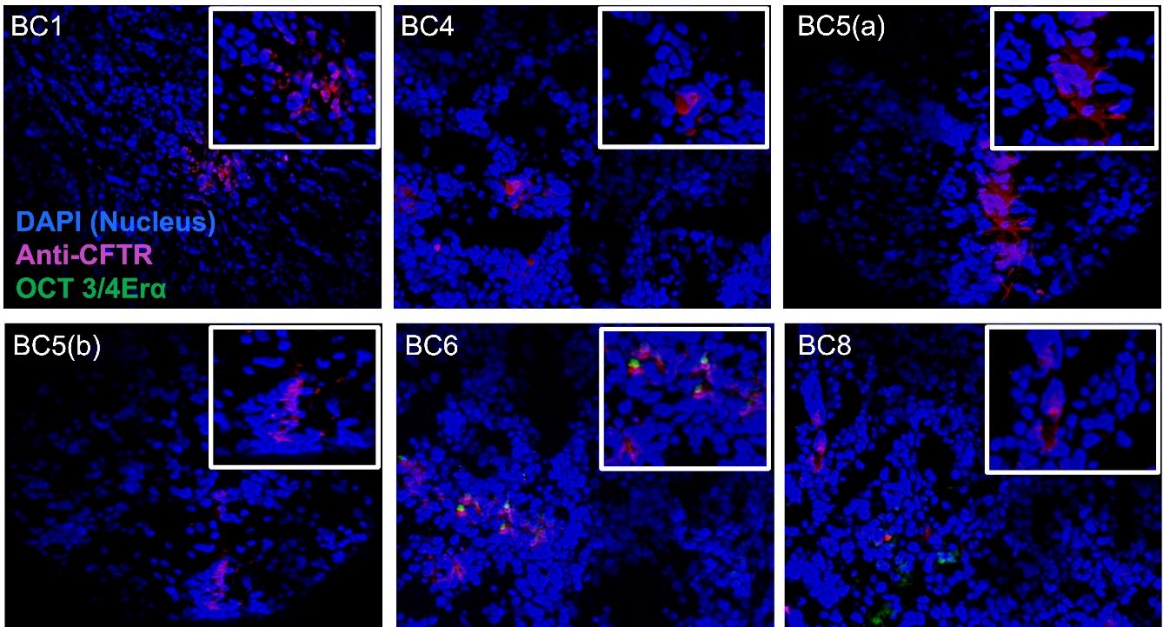

Figure 3 CFTR expression in high-grade tumors. Images referenced above are sourced from grade III metastatic tumors. We used DAPI for nuclei visualization. CFTR and Oct3/4 were the antibodies used for biomarkers visualization. The primary and secondary antibodies were used at concentrations of 1:200 and 1:500, respectively. As shown, CFTR expression in red was low in high-grade tumors. Images showed CFTR expression at all three places, i.e., cell membrane, cytoplasm, and inside the nucleus, which confirms defective CFTR presence in high-grade tumors. Somewhere CFTR expression was found in the nucleus too. Since CFTR only expresses in the cytoplasm (organelles) and at the cell membrane, the possible reason for CFTR expression in the nucleus is that, while taking the images, CFTR expressing organelle happened to be on the top of that nucleus. The image also shows fragments of CFTR scattered in the cytoplasm of the cell, which shows that CFTR synthesis was not normal, and it broke down into fragments in the cytoplasm before reaching the cell membrane. At the same time, red signals in the form of lines show CFTR expression on cell membranes.

3.2.3. CFTR Expression in ER+ Tumors

Furthermore, for the evaluation of the relationship between CFTR expression and estrogen receptor alpha (ER+) status, immunofluorescence staining was conducted on three BC tissue samples (BC3, BC7, and BC10). Based on previous testing, these samples were identified as ER+ and were selected to provide insights into the role of CFTR in ER+ BC. Figure 4 documents these findings.

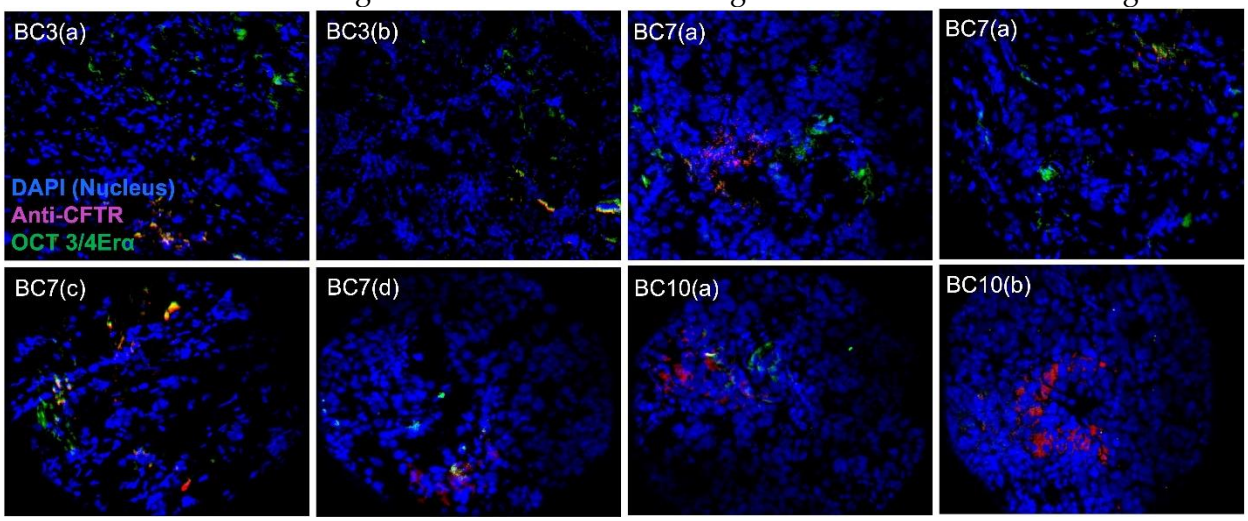

Figure 4 CFTR expression in estrogen receptor-positive tumors. Immunofluorescence staining on ER+ tumors gave the results mentioned above. We used DAPI for nuclei visualization. CFTR and ER alpha antibodies from Abcam were used against CFTR and estrogen protein. The primary and secondary antibodies were used at concentrations of 1:200 and 1:500, respectively. Compared to high-grade tumors, the expression of CFTR (represented in red) was not low in ER+ tumors. CFTR is expressed in the cytoplasm and at the cell membrane. In some instances, both CFTR and estrogen receptor alpha were expressed together, resulting in a yellowish color created by the combination of red and green. The estrogen receptor alpha was expressed in the nucleus and cytoplasm.

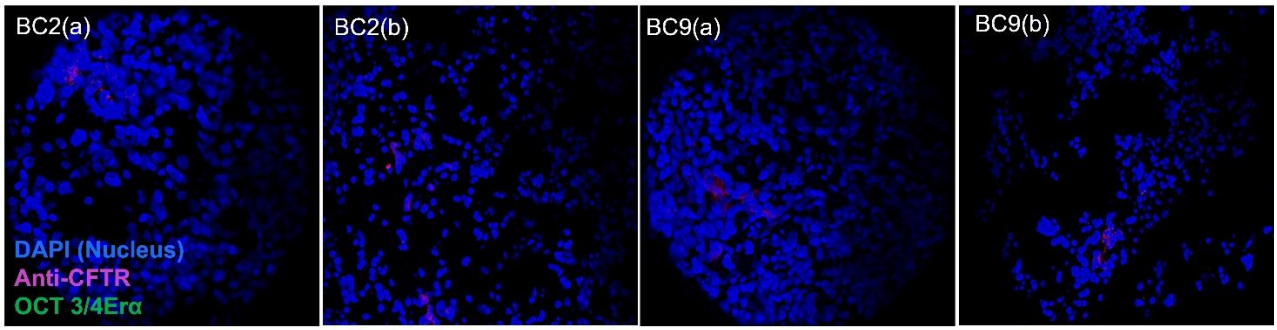

Figure 5. CFTR expression in triple-negative BC tumors. DAPI and CFTR staining on TNBC tumors produced the results shown above. In one sample, we did not detect any CFTR expression; in another, the expression was very low. CFTR was expressed in the cytoplasm in fragmented fo123456rm, indicating an abnormal presence of CFTR in triple-negative BC.

3.2.4. CFTR Expression in TNBC

To detect CFTR expression in TNBC, immunofluorescence staining was conducted on TNBC tissue, i.e., BC2 and BC9, depicted in Figure 5.

3.2.5. Biomarkers Expression Counting

Nuclei and expressed biomarkers were counted both manually and automatically. We counted the percentages of expressed biomarkers from these values, and the mean was taken. We calculated the standard deviation and standard error mean from calculating the mean. As shown, the length of the error bar is significantly less, which means that the data was precise.

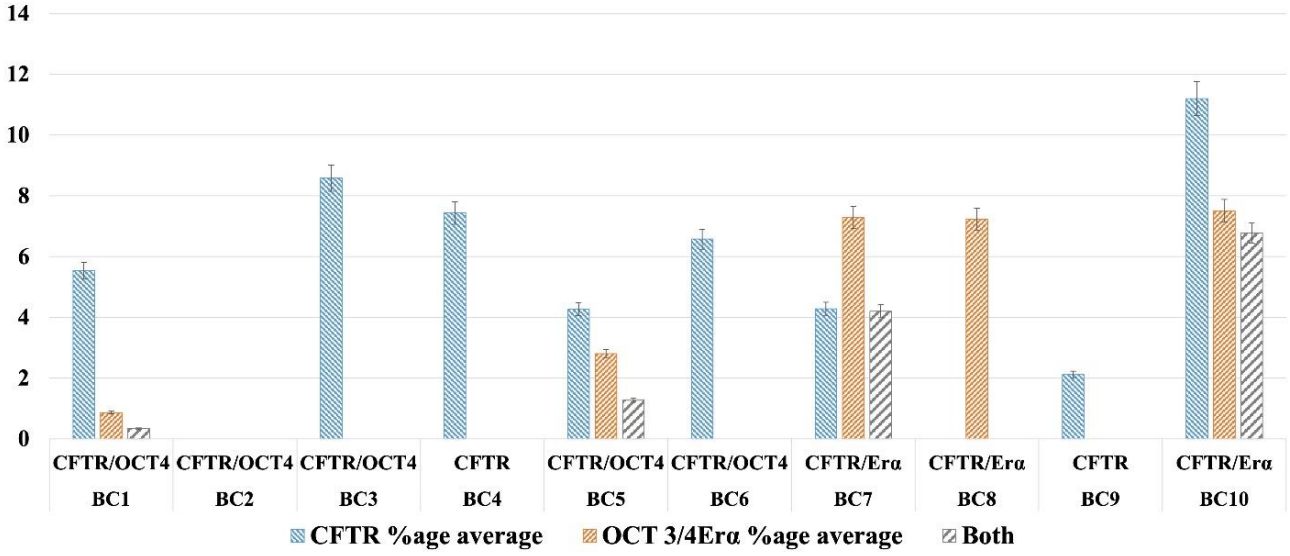

Patient ID$^{\text{Tumor Type}}_{\text{Grade}}$	Antibodies used	CFTR %age average	OCT 3/4Erα %age average	Both
$BC1^{III}_{ER/PR+}$	CFTR/OCT4	5.54	0.865	0.34
$BC2^{III}_{TNBC}$	CFTR/OCT4	0	0	0
$BC3^{II}_{ER+}$	CFTR/OCT4	8.585	0	0
$BC4^{III}_{ER/PR+}$	CFTR	7.44	0	0
$BC5^{III}_{ER/PR+}$	CFTR/OCT4	4.265	2.8	1.27
$BC6^{III}_{ER/PR/HER2+}$	CFTR/OCT4	6.575	0	0
$BC7^{II}_{ER+}$	CFTR/Erα	4.28	7.290	4.20
$BC8^{III}_{ER/PR+}$	CFTR/Erα	0	7.235	0
$BC9^{III}_{TNBC}$	CFTR	2.12	0	0
$BC10^{II}_{ER+}$	CFTR/Erα	11.205	7.51	6.78

Figure 6. Summary of the biomarkers' expression in different types of BC samples.

4. Discussion

Although several abnormalities and toxicity issues in BC patients have been reported, yet little is done to repurpose a noncancerous and less toxic FDA-approved drug to treat it (Aggarwal et al. 2021). Studies on the role of ion channels, like CFTR, in BC are minimal. In the present study, we analyzed CFTR expression in different types of BC through immunofluorescence staining. Consequently, we found some noncancerous FDA-approved agonists and antagonists for repurposing.

One notable example of drug repurposing is chemotherapeutic mitotic inhibitors, i.e., docetaxel, paclitaxel, and vinblastine, now used in cancer. Interestingly, paclitaxel was discovered in 1971 to manage arterial restenosis (Roberts 2020). These drugs have demonstrated efficacy in their primary indications and in affecting mitotic activity and inducing programmed cell death (apoptosis) in cancer cells by targeting bcl2 *(Acharya et al. 2019).* Similarly, our study suggests potential drugs for repurposing in BC.

In-silico drug repurposing has yielded many success stories. For example, EGFR3 is a well-known protein biomarker in bladder cancer; Ke and his colleagues demonstrated its inhibition by six compounds through computational methods. The success rate was two compounds, validated in-vitro, while others showed efficacy in a xenograft mouse model (Ke et al. 2017). Similarly, in our study, we docked 11 drugs with the target protein CFTR and identified glyburide, tezacaftor, and lumacaftor, as the most promising drugs for potential repurposing in BC.

Moreover, we identified a protein called CFTR after extensive text mining and using different databases, including "the repurposing hub," "gene card," "uniport", and "human protein atlas." A list of fifty drugs and their targets was obtained and subjected to exclusion-inclusion criteria. Drug-based protein identification was done for all the drugs and their targets by searching the repurposing database. This method led to the identification of an unusual biomarker called CFTR. The same hub was searched again to obtain all the drugs that target CFTR. Similar strategies utilizing protein libraries have been mentioned by Ram Samudrala and William Mangione(Chi et al. 2019), in 2019, showcasing their application in discovering promising drugs for various diseases. Additionally, text mining has been highlighted by Fleuren et al. as a valuable tool for exploring different relations and acquiring relevant knowledge in drug repositioning (Saha Roy and Vadlamudi 2012; Hunter et al. 2010).

While docking CFTR with a list of 11 drugs, we selected a crystal structure 6O2P for CFTR, which was in conjugation with a suitable ligand, as the ligand specifies suitable binding sites for drug binding (Krisnamurti and Fatchiyah 2019). 6O2P was a mutant type of protein because defective CFTR is implicated in BC progression (Elokely and Doerksen 2013). A similar approach was followed by H. R. Bhojwani and U. J. Joshi in the year 2019 when selecting the crystal structure 4ASE for VEGFR-2 (Bhojwani and Joshi 2019).

For docking studies, we first identified the binding site residues of CFTR through different databases where drugs were supposed to bind. These residues were F932, S308, Y304, F305, F236, L233, A309, F931, G930, F312, and VX71512. These results were consistent with the work of *Giada Righetti et al.*, who, in the year 2020, showed F236, Y304, F305, F312, F931, Y304, and S308 as the active site of CFTR (Righetti et al. 2020).

Before docking, the docking protocol was validated by using RMSD. Our redocked drug was found almost exactly superimposed on the experimental structure with an RMSD value of

0.4531 Å, indicating a close agreement between the redocked and experimental structure. This validation ensures the reliability of the docking protocol and allows for further docking experiments. A similar approach was used by Mohammad Firoz Khan et al.when redocking celecoxib into the COX-2 crystal structure, which validated their docking protocol for subsequent studies(Khan et al. 2015). In obtained results, both drugs were superimposed with RMSD value below 1, which validates their docking protocol, and then used this protocol for their study.

In our study, we suggested the top three drugs for repurposing based on docking score. These drugs had lower binding energy values, i.e., -20.6541, -20.0947, and -19.1977 for glyburide, tezacaftor, and lumacaftor, respectively. Similarly, *Reetuparna Acharya et.al.,* through docking studies in 2019, showed XAN, BER, ANG, PSO, and IMP as powerful anticancer agents (Acharya et al. 2019). This was further confirmed by in-vitro analysis. *Giada Righettiet.al.* 2020 docked lumacaftor and its structurally similar compound with CFTR; they concluded that lumacaftor binds to CFTR with the lowest binding energy, i.e., -21.04 (Righetti et al. 2020). While in our results, lumacaftor and CFTR complex showed a -19.1977 binding score.

Glyburide, tezacaftor, and lumacaftor, the top-ranked drugs in our study, are known for their antagonist and agonist actions on CFTR, respectively. Since CFTR overexpression was found to play an important role in the progression of ovarian cancer by increased estrogen production (Xu et al. 2015), glyburide as an antagonist may play an important role in BC prognosis by down-regulating or inhibiting CFTR action (Abraham et al. 1996), while both tezacaftor and lumacaftor work as an agonist in cystic fibrosis by correcting CFTR functioning(Lopes-Pacheco 2020). As down-regulation of CFTR was found to be involved in BC metastasis (Zhong et al. 2014), so both drugs can work as agonists in BC by stopping EMT in BC.

Besides a key role in BC, Estrogen signaling plays a vital role in normal breast cell growth and differentiation (Chi et al. 2019). The abnormal signaling inside and outside the cells can potentially promote metastasis in ER-positive BC(Saha Roy and Vadlamudi 2012). Out of ten cases in our study, three samples were ER+ tumors, i.e., BC3, BC7, and BC10. Hui Chen et al. in 2012 showed CFTR involvement in regulating estrogen production in ovaries via FSH stimulated signaling pathway. This finding of CFTR-based amplification of hormonal response may also be valid in organs other than ovaries (Chen et al. 2012). So to check the relation between CFTR and Estrogen production, we applied both the antibodies, i.e., anti-CFTR and anti-estrogen receptor alpha, to BC7 and BC 10 and only CFTR antibody to BC3. CFTR-expressing cells in BC7 were 4.28%, estrogen receptor alpha-expressing cells were 7.67%, and cells expressing both biomarkers were 4.20 %. Similarly, in BC10, CFTR-expressing cells were 11.20 % while ER alpha-expressing cells were 7.51%, and cells expressing both the biomarkers were 6.78%, which means that here in BC, there might be some relation between the both. These findings contradict the results of Jie Ting Zhang et al., who found that CFTR expression is unrelated to ER/PR status.

In almost all our results, defective, fragmented CFTR expression was found in the cytoplasm. These results were consistent with the study of *Jie Ting Zhang et al.,* who reported abnormal CFTR expression in BC and its inverse relation to poor prognosis(Zhang et al. 2013). Our results also showed defective CFTR expression on the apical membrane, which aligns with the findings of Hunter MJ et al. (2010), who showed

that defective CFTR presence on the apical membrane leads to NF-κB activation. NFκB activation, in turn, results in overproduction of cytokines, contributing to inflammation (Hunter et al. 2010). Also, Huber and co-workers in 2004 worked on NFκB and identified its central role in EMT using a BC mouse model(Huber et al. 2004).

EMT is a fundamental multistep process step involved in spreading cancer to distant organs and is characterized by tumor cells' motility and invasion (Liu et al. 2020). *Xie C and fellows* found that CFTR regulates the transcriptional factor NF-κB. (Xie et al. 2013) . Overexpression of this protein will lead to abnormal activation of a complex called the uPA/uPAR axis, which is critical in EMT. This results in the loss of cell integrity and disruption of tight junctions, promoting the motility of cancerous cells(Muriithi et al. 2020). In all five samples, i.e., BC1, BC4, BC5, BC6, and BC8, CFTR expression did not exceed 8%, indicating down-regulation of CFTR and its potential involvement in cancer progression and aggressiveness. Xie C et al. (Xie et al. 2013) reported similar findings in 2012, where CFTR was downregulated in prostate cancer, and CFTR overexpression suppressed uPA/uPAR expression. They also showed that inhibition of CFTR promoted proliferation, cell invasion, and migration in xenograft mouse models with prostate cancer. In the same way, Liu C *et al.* in the year 2020 (Liu et al. 2020) conducted research work to find out CFTR function in colorectal cancer and found CFTR expression to be down-regulated in cancerous tissues.

Lastly, Liu K, Dong F, et al. (2013, 2020) reported CFTR DNA methylation to be involved in TNBC cell lines. Treatment with DNA methylation inhibitors was found to be effective in rescuing CFTR mRNA (Zhang et al. 2013; Liu et al. 2020). In our case, two codes were TNBC cases. BC2, an FFPE sample, showed no CFTR expression, while BC9, a frozen sample, showed minimal CFTR expression. The finding that CFTR is expressed in BC samples and that various drugs can potentially target CFTR for BC treatment warrants future in vivo and in vitro experiments on drug repurposing in BC.

5. Conclusions

Our study represents an initial stride towards conducting in vitro and in vivo experiments focusing on repurposing CFTR-targeting drugs for treating BC. Specifically, we explored the potential of glyburide to inhibit CFTR and subsequently suppress estrogen production while investigating how tezacaftor can enhance CFTR action to counteract tumor aggressiveness.

Conflict of Interest

The authors declare that they have no competing interests.

Funding

This study was funded by the Higher Education Commission of Pakistan under the NRPU grant no. HEC/NRPU/6820/2016. In addition, we gratefully acknowledge the financial support provided by ORIC (Office of Research, Innovation, and Commercialization) and the Institute of Basic Medical Sciences at Khyber Medical University, Peshawar.

Study Approval

This study was approved by the ethical committee of Khyber Medical University, and Khyber teaching hospital, Peshawar.

Consent Forms

Consent forms are available with the authors.

Data Availability

All the data related to this study are available with the authors.

Authors Contribution

INK and AA conceptualized and supervised the study, MMK provided surgical samples, SR, SK, SW, HN, and SF helped in the bench work, and analysis. BJ helped in analyzing the docking study. All authors helped in improving and writing of drafted manuscript, edited and approved for publication.

Acknowledgment

We sincerely thank our colleagues at the Cancer Cell Culture & Precision Oncomedicine Lab for their invaluable technical assistance throughout this research project.

References

Abraham, Edward H., Petra Vos, Julia Kahn, Shelley A. Grubman, Douglas M. Jefferson, Ivan Ding, and Paul Okunieff. 1996. "Cystic fibrosis hetero–and homozygosity is associated with inhibition of breast cancer growth." *Nature medicine* 2: 593–596.

Acharya, Reetuparna, Shinu Chacko, Pritha Bose, Antonio Lapenna, and Shakti Prasad Pattanayak. 2019. "Structure based multitargeted molecular docking analysis of selected furanocoumarins against breast cancer." *Scientific reports* 9: 1–13.

Aggarwal, Sadhna, Sumit Singh Verma, Sumit Aggarwal, and Subash Chandra Gupta. 2021. "Drug repurposing for breast cancer therapy: Old weapon for new battle." Seminars in cancer biology.

Ahmed, Aliyu Hamidu, and Yusuf Ibrahim Alkali. 2019. "In silico pharmacokinetics and molecular docking studies of lead compounds derived from Diospyros mespiliformis." *PharmaTutor* 7: 31–37.

Antoszczak, Michał, Anna Markowska, Janina Markowska, and Adam Huczyński. 2020. "Old wine in new bottles: Drug repurposing in oncology." *European Journal of Pharmacology* 866: 172784.

Bairoch, Amos, Rolf Apweiler, Cathy H. Wu, Winona C. Barker, Brigitte Boeckmann, Serenella Ferro, Elisabeth Gasteiger, Hongzhan Huang, Rodrigo Lopez, Michele Magrane, and others. 2005. "The universal protein resource (UniProt)." *Nucleic acids research* 33: D154–D159.

Bhojwani, H. R., and U. J. Joshi. 2019. "Selecting protein structure/s for docking-based virtual screening: A case study on type II inhibitors of VEGFR-2 kinase." *Int. J. Pharm. Sci. Res* 10: 2998–3011.

Cao, Wei, Hong-Da Chen, Yi-Wen Yu, Ni Li, and Wan-Qing Chen. 2021. "Changing profiles of cancer burden worldwide and in China: a secondary analysis of the global cancer statistics 2020." *Chinese Medical Journal* 134: 783–791.

Chen, Hui, Jing Hui Guo, Yong Chao Lu, Guo Lian Ding, Mei Kuen Yu, Lai Ling Tsang, Kin Lam Fok, Xin Mei Liu, Xiao Hu Zhang, Yiu Wa Chung, and others. 2012. "Impaired CFTR-dependent amplification of FSH-stimulated estrogen production in cystic fibrosis and PCOS." *The Journal of Clinical Endocrinology & Metabolism* 97: 923–932.

Chi, David, Hari Singhal, Lewyn Li, Tengfei Xiao, Weihan Liu, Matthew Pun, Rinath Jeselsohn, Housheng He, Elgene Lim, Raga Vadhi, and others. 2019. "Estrogen receptor signaling is

reprogrammed during breast tumorigenesis." *Proceedings of the National Academy of Sciences* 116: 11437–11443.

Cohen, Taylor Sitarik, and Alice Prince. 2012. "Cystic fibrosis: a mucosal immunodeficiency syndrome." *Nature medicine* 18: 509–519.

El-Hamamsy, Mervat H. 2017. "Accessing the anti-proliferating activity of tankyrase-2 inhibitors via 2d, 3d-QSAR and molecular docking: assessment of structure activity relationships." *Journal of Applied Pharmaceutical Science* 7 (12): 014-027.

Elokely, Khaled M., and Robert J. Doerksen. 2013. "Docking challenge: protein sampling and molecular docking performance." *Journal of chemical information and modeling* 53: 1934–1945.

Huber, Margit A., Ninel Azoitei, Bernd Baumann, Stefan Grünert, Andreas Sommer, Hubert Pehamberger, Norbert Kraut, Hartmut Beug, Thomas Wirth, and others. 2004. "NF-κB is essential for epithelial-mesenchymal transition and metastasis in a model of breast cancer progression." *The Journal of clinical investigation* 114: 569–581.

Hunter, Mairi J., Kate J. Treharne, Alexandra K. Winter, Diane M. Cassidy, Stephen Land, and Anil Mehta. 2010. "Expression of wild-type CFTR suppresses NF-κB-driven inflammatory signalling." *PloS one* 5: e11598.

Ke, Kunbin, Hongjian Li, Hong Yao, Xi-Nan Shi, Chao Dong, Ying Zhu, Xu Liu, Ling Li, Kwong-Sak Leung, Man-Hon Wong, and others. 2017. "In silico prediction and in vitro and in vivo validation of acaricide fluazuron as a potential inhibitor of FGFR 3 and a candidate anticancer drug for bladder carcinoma." *Chemical Biology & Drug Design* 89: 505–513.

Khan, Mohammad Firoz, Sabreena Aleem Nabila, Ridwan Bin Rashid, Mohammad Sharifur Rahman, Abu Asad Chowdhury, and Mohammad Abdur Rashid. 2015. "In silico molecular docking studies of lichen metabolites against cyclooxygenase-2 enzyme." *Bangladesh Pharmaceutical Journal* 18: 90–96.

Krisnamurti, G. C., and F. Fatchiyah. 2019. "Interaction of acetaminophen and caffeine towards cyclooxygenase-2 (COX-2) in inhibition of prostaglandin (PGH2) synthesis." Journal of Physics: Conference Series.

Li, Yafei, Zhifu Sun, Yanhong Wu, Dusica Babovic-Vuksanovic, Yan Li, Julie M Cunningham, Vernon S Pankratz, and Ping Yang. 2010. "Cystic fibrosis transmembrane conductance regulator gene mutation and lung cancer risk." *Lung cancer* 70 (1): 14-21.

Liu, Can, Chao Song, Jiaxi Li, and Qing Sun. 2020. "CFTR functions as a tumor suppressor and is regulated by DNA methylation in colorectal cancer." *Cancer Management and Research* 12: 4261.

Locher, Kaspar P. 2016. "Mechanistic diversity in ATP-binding cassette (ABC) transporters." *Nature structural & molecular biology* 23: 487–493.

Lopes-Pacheco, Miquéias. 2020. "CFTR modulators: the changing face of cystic fibrosis in the era of precision medicine." *Frontiers in pharmacology*: 1662.

Meng, Xin, Jack Clews, Anca D. Ciuta, Eleanor R. Martin, and Robert C. Ford. 2019. "CFTR structure, stability, function and regulation." *Biological chemistry* 400: 1359–1370.

Muriithi, Wanjiru, Lucy Wanjiku Macharia, Carlos Pilotto Heming, Juliana Lima Echevarria, Atunga Nyachieo, Paulo Niemeyer Filho, and Vivaldo Moura Neto. 2020. "ABC transporters and the hallmarks of cancer: roles in cancer aggressiveness beyond multidrug resistance." *Cancer Biology & Medicine* 17: 253.

Pinzi, Luca, Christian Lherbet, Michel Baltas, Federica Pellati, and Giulio Rastelli. 2019. "In silico repositioning of cannabigerol as a novel inhibitor of the enoyl acyl carrier protein (ACP) reductase (INHA)." *Molecules* 24: 2567.

Polamreddy, Prasanthi, and Nandu Gattu. 2019. "The drug repurposing landscape from 2012 to 2017: evolution, challenges, and possible solutions." *Drug Discovery Today* 24: 789–795.

Qiao, Di, Long Yi, Lixin Hua, Zheng Xu, Yi Ding, Dongquan Shi, Ligang Ni, Ninghong Song, Yong Wang, and Hongfei Wu. 2008. "Cystic fibrosis transmembrane conductance regulator (CFTR) gene 5T allele may protect against prostate cancer: a case-control study in Chinese Han population." *Journal of Cystic Fibrosis* 7 (3): 210-214.

Quintana-Gallego, Esther, Isabel Delgado-Pecellín, and Carmen Calero Acuña. 2014. "CFTR protein repair therapy in cystic fibrosis." *Archivos de Bronconeumología (English Edition)* 50: 146–150.

Rangel-Vega, Adrián, Lawrence R. Bernstein, Edna-Ayerim Mandujano Tinoco, Silvia-Julieta García-Contreras, and Rodolfo García-Contreras. 2015. "Drug repurposing as an alternative for the treatment of recalcitrant bacterial infections." *Frontiers in microbiology* 6: 282.

Righetti, Giada, Monica Casale, Nara Liessi, Bruno Tasso, Annalisa Salis, Michele Tonelli, Enrico Millo, Nicoletta Pedemonte, Paola Fossa, and Elena Cichero. 2020. "Molecular docking and QSAR studies as computational tools exploring the rescue ability of F508del CFTR correctors." *International journal of molecular sciences* 21: 8084.

Roberts, Andrew W. 2020. "Therapeutic development and current uses of BCL-2 inhibition." *Hematology 2014, the American Society of Hematology Education Program Book* 2020: 1–9.

Saha Roy, Sudipa, and Ratna K. Vadlamudi. 2012. "Role of estrogen receptor signaling in breast cancer metastasis." *International journal of breast cancer* 2012.

Thul, Peter J., and Cecilia Lindskog. 2018. "The human protein atlas: a spatial map of the human proteome." *Protein Science* 27: 233–244.

Toprak, Demet, Chelsea Davis, and Margaret Rosenfeld. 2019. "Treating the Airway Consequences of Cystic Fibrosis Transmembrane Conductance Regulator Dysfunction." Seminars in Respiratory and Critical Care Medicine.

Warren, N, JA Holmes, L Al-Jader, RR West, DC Lewis, and RA Padua. 1991. "Frequency of carriers of cystic

fibrosis gene among patients with myeloid malignancy and melanoma." *BMJ: British Medical Journal* 302 (6779): 760.

Xie, C. F. T. R., X. H. Jiang, J. T. Zhang, T. T. Sun, J. D. Dong, Andrew James Sanders, R. Y. Diao, Y. Wang, K. L. Fok, L. L. Tsang, and others. 2013. "CFTR suppresses tumor progression through miR-193b targeting urokinase plasminogen activator (uPA) in prostate cancer." *Oncogene* 32: 2282–2291.

Xu, Jiao, Min Yong, Jia Li, Xiaojing Dong, Tinghe Yu, Xiao Fu, and Lina Hu. 2015. "High level of CFTR expression is associated with tumor aggression and knockdown of CFTR suppresses proliferation of ovarian cancer in vitro and in vivo." *Oncology Reports* 33: 2227–2234.

You, Jie-shu, Li Guo, Mei Huang, Xin-lei Shi, Man-di Lin, Zhen Guo, Ya-li Cao, You-zhi Sun, Qian Xu, Wei-ling Qu, and others. 2019. "The effect and mechanism of YH0618 granule on chemotherapy-induced hair loss in patients with breast cancer: study protocol for a randomized, double-blind, multi-center clinical trial." *Trials* 20: 1–8.

Zhang, Jie Ting, Xiao Hua Jiang, Chen Xie, Hong Cheng, Jian Da Dong, Yan Wang, Kin Lam Fok, Xiao Hu Zhang, Ting Ting Sun, Lai Ling Tsang, and others. 2013. "Downregulation of CFTR promotes epithelial-to-mesenchymal transition and is associated with poor prognosis of breast cancer." *Biochimica et Biophysica Acta (BBA)-Molecular Cell Research* 1833: 2961–2969.

Zhong, Hai-Jing, Li-Juan Liu, Daniel Shiu-Hin Chan, Hui-Min Wang, Philip Wai Hong Chan, Dik-Lung Ma, and Chung-Hang Leung. 2014. "Structure-based repurposing of FDA-approved drugs as inhibitors of NEDD8-activating enzyme." *Biochimie* 102: 211–215.

Zhu, Q., H. Li, Y. Liu, and L. Jiang. 2017. "Knockdown of CFTR enhances sensitivity of prostate cancer cells to cisplatin via inhibition of autophagy." *Neoplasma* 64: 709–717.